Eur. Phys. J. B **13**, 701–705 (2000)

THE EUROPEAN PHYSICAL JOURNAL B

EDP Sciences

Plasmons in icosahedral quasicrystals: An EELS investigation

T. Grenet[1,a] and M.C. Cheynet[2]

[1] LEPES-CNRS, 25 avenue des Martyrs, BP 166, 38042 Grenoble Cedex 9, France
[2] LTPCM, 1130 rue de la piscine, Domaine Universitaire, BP 75, 38402 Saint Martin d'Hères Cedex, France

Received 3 November 1998 and Received in final form 16 July 1999

Abstract. We present the results of an electron energy loss spectroscopy (EELS) investigation of the icosahedral quasicrystals i-Al-Cu-Fe, i-Al-Pd-Mn and i-Al-Pd-Re. The spectra of the three systems studied are very similar. Their main contribution comes from a broad plasmon like peak, which can be interpreted as an "$s-p$" electron plasmon damped by "d" electron interband transitions. We show that it is similar to those found in other simple crystalline aluminum-transition metal alloys, so that no specificity related to the quasicrystalline order of the alloys dominates.

PACS. 71.23.Ft Quasicrystals – 71.45.Gm Exchange, correlations, dielectric and magnetic functions, plasmons

1 Introduction

Quasicrystals display surprising electronic properties, mostly exemplified by their electrical transport [1]. Icosahedral alloys such as i-Al-Cu-Fe or i-Al-Pd-Re have very high resistivities. The latter, in spite of displaying a relatively high density of states at the Fermi level (according to low temperature specific heat data), is believed to cross a metal to insulator transition, which is unique for highly ordered alloys of metals.

There are still few studies of the conductivity (or dielectric constant) of quasicrystals as a function of frequency. Reflectivity measurements were performed, which give access to $\sigma(\omega)$ in the infrared to close ultraviolet range [2]. The main result for the icosahedral quasicrystals and the decagonal ones along the quasiperiodic axis, is the absence of Drude peak at low energy, and a broad absorption at around 1–2 eV, which was interpreted as a signature of interband transitions across a pseudogap.

Electron energy loss spectroscopy (EELS) can give access to the dielectric constant at higher energy and is thus complementary to optical studies. EELS measurements were performed in icosahedral i-Al-Mn-(Si) [3–5], i-Al-Pd-Mn [6,7], i-Al-Cu-Ru [8] alloys and recently in decagonal d-Al-Ni-Co and d-Al-Ni-Rh alloys [9]. All the spectra display an intense peak around 16–19 eV. While it was interpreted as a free electron like plasmon excitation in [4,8,9], it was suggested by other authors that such a plasmon should be anomalously damped or even absent in quasicrystals, and experimental data on icosahedral i-Al-Mn and i-Al-Pd-Mn were discussed within this framework [3,6,7], based on the peculiar band structure and electronic properties of icosahedral quasicrystals.

[a] e-mail: grenet@lepes.polycnrs-gre.fr

In this paper we present EELS measurements in the 0–50 eV range performed on the stable icosahedral alloys i-Al-Cu-Fe, i-Al-Pd-Mn and i-Al-Pd-Re. We discuss the nature of the strong signal observed and argue that it corresponds to a $s-p$ electron volume plasmon excitation. Data and interpretations given in the literature mentioned above about i-Al-Pd-Mn are discussed. We compare the experimental data on quasicrystals to the ones on some simple crystalline aluminium-transition metal alloys, and conclude that, according to the existing experimental data, plasmon excitations in quasicrystals do not exhibit clear features related to quasiperiodicity.

2 Experimental procedure

Samples of nominal compositions $Al_{62.5}Cu_{25}Fe_{12.5}$ and $Al_{70.5}Pd_{21}Re_{8.5}$ were prepared as melt spun ribbons and annealed at high temperature [10], and a piece of i-$Al_{68}Pd_{23}Mn_9$ was cut from a single grain grown by the Czochralski method. For the EELS measurements, the samples were ground into fine particles and deposited on copper grids covered with holed carbon films. Only the particles with a thickness $t < 50$ nm for which the thin parts were located over an hole were analyzed. The measurements were performed using either a Vacuum Generator HB501 and a Philips CM20 FEG scanning transmission electron microscopes, fitted with a [310] tungsten tip and a LaB6 filament respectively, and operating at 100 kV for the HB 501 and 200 kV for the CM20. The HB 501 is connected to a serial detector (EL80-VG), whereas the CM20 is connected to a parallel one (Gatan 666), corresponding to instrumental resolutions respectively equal to 0.4 ± 0.05 eV and to 0.8 ± 0.1 eV. Because the inelastic

scattering signal is concentrated into a small scattering angle, α – the illumination angle of the specimen – and β – the collection angle of the spectrometer – had to be selected so as to collect the signal in a scattering angle as small as possible [11,12], the conditions chosen were 9.33 mrad for α and 0.7 mrad for β, corresponding to a 2 nm probe diameter and a maximum scattering vector $q_{\max} = 0.331$ Å^{-1}. In the case of the i-Al-Cu-Fe alloy, $q_{\max}$ was increased up to 2.24 Å^{-1} without any significant alteration of the spectra. Thus when extracting the width of the loss peaks, no correction for dispersion effects was performed. The spectra were recorded on a 50 eV energy width corresponding to an energy dispersion of 0.05 eV per channel. The acquisition duration at the same place was fixed to 20 seconds to limit contamination and irradiation damages induced by the electron probe. Each analyzed particle was imaged and its structure checked by electron diffraction before its spectrum was recorded. Pure Al particles were used to calibrate the spectrometer, the Al plasmon peak position was then fixed equal to 15.1 eV. For each icosahedral system tens of spectra were recorded under the same experimental conditions and treated to extract the results reported and discussed below.

The FWHM and the energy of the plasmon peaks were determined according to the following procedure: the FWHM of the experimental elastic peak was first measured, then the single scattering signal was extracted from the experimental spectrum using the Fourier-Log deconvolution routine of EL/P software [12], and the FWHM of the main peak was deduced from a fitting of this spectrum with a Lorentzian curve using the ABFfit software [13]. The FWHM of the plasmon peak was then defined as the FWHM of the single scattering peak minus the FWHM of the zero-loss peak of the experimental spectrum.

The real part $\mathrm{Re}(\varepsilon)$ and the imaginary part $\mathrm{Im}(\varepsilon)$ of the dielectric function were derived from a Kramer-Kronig analysis of the loss function normalized to match the condition $\mathrm{Re}(1/\varepsilon(E=0)) = 0$, using a subroutine-package attached to the Mathematica-software [14]. The loss functions were obtained from the experimental spectra after substraction of the zero-loss peak and deconvolution of the plural scattering effects. The deconvolution of the elastic scattering is a rather difficult operation [15] because the zero-loss peak is never perfectly symetric and can have a "high energy tail" (imperfect focusing of the spectrum onto the detector or slight shifts of the data during the collection may contribute). A discontinuity then results when the zero loss peak is substracted. In this work the discontinuity located around 4 eV, was smoothed out with a Ax^{-n} function applied between about 4 eV to 0 eV. In addition the loss function was extended on the high energy side using a Lorentzian tail to improve the FFT calculations involved in the single loss spectra calculations.

3 Experimental results

In Figure 1 we show a typical experimental spectrum recorded from the i-Al-Cu-Fe sample and the corresponding loss function. The spectra of i-Al-Pd-Mn and i-Al-Pd-Re are very similar. Among the tens of spectra measured, special care was taken to identify and eliminate those containing signs of high carbon or oxygen contamination prior to any other processing. On the low-loss spectrum, these contaminants may cause spurious signals located around 6–7 eV and 23–24 eV [16,17].

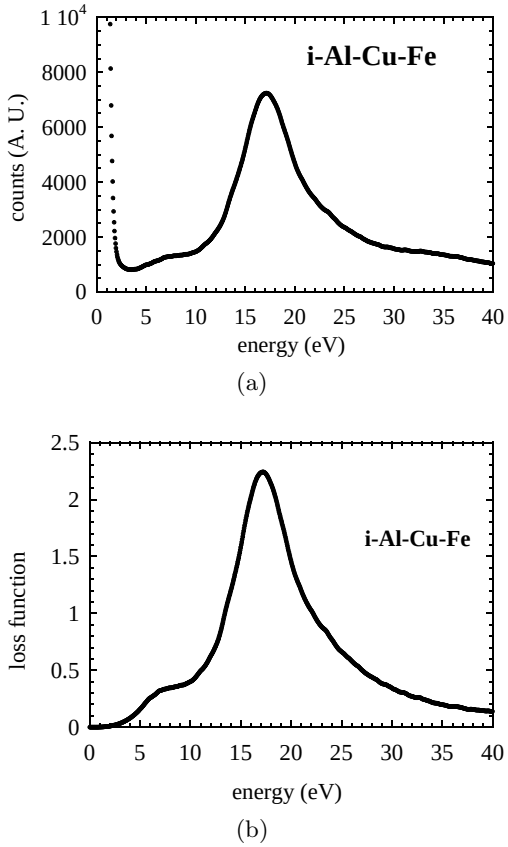

Fig. 1. (a) Electron energy loss spectrum and (b) loss function $\mathrm{Im}[-1/\varepsilon(E)]$ of i-$Al_{62.5}Cu_{25}Fe_{12.5}$.

Table 1. Energy and full width at half maximum of the main loss peaks of the i-$Al_{62.5}Cu_{25}Fe_{12.5}$, i-$Al_{68}Pd_{23}Mn_9$ and i-$Al_{70.5}Pd_{21}Re_{8.5}$ alloys.

	i-Al-Cu-Fe	i-Al-Pd-Mn	i-Al-Pd-Re
E_{p} (eV)	16.9 ± 0.3	16.8 ± 0.3	17.2 ± 0.5
$\delta E_{1/2}$ (eV)	5.3 ± 0.4	6.1 ± 0.5	6.3 ± 0.6

Apart from the elastic peak, a typical spectrum mainly consists of an intense broad and asymmetric signal, which maximum is located around 17 ± 1 eV. Double losses are also sometimes observed with intensities depending on the particles thickness. In Table 1, we give the main peak energy (E_{p}) and the full width at half maximum ($\delta E_{1/2}$) corresponding to each system evaluated as described in the preceding section. It has to be noted that for all the i-Al-Fe-Cu spectra and for i-Al-Pd-Mn or i-Al-Pd-Re spectra, but with a weaker intensity, a bump located at around

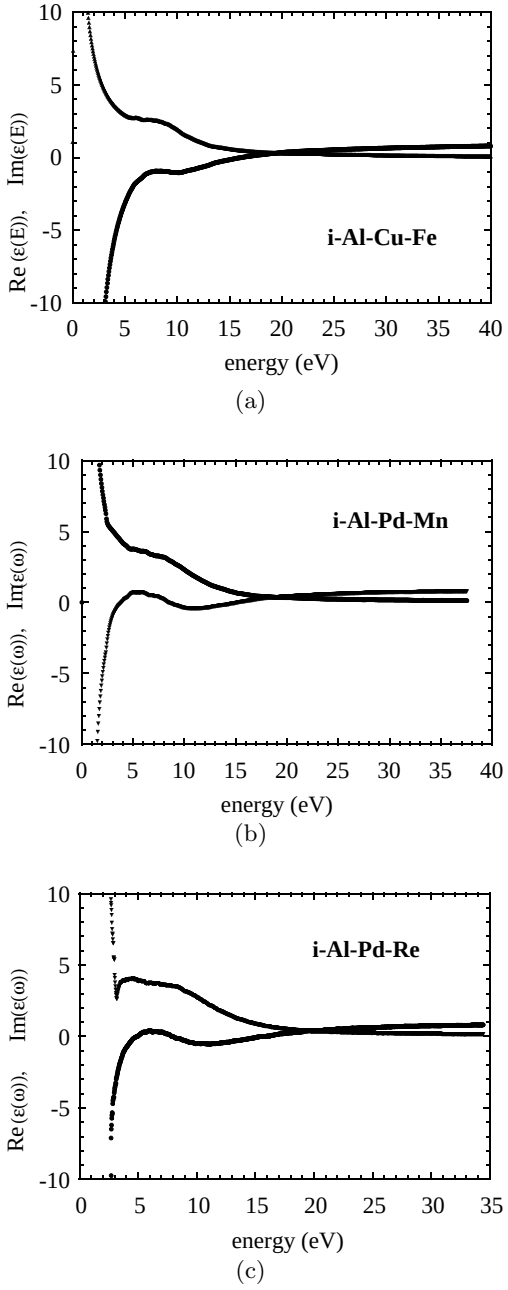

Fig. 2. Real and imaginary parts of the dielectric constant of: (a) i-$Al_{62.5}Cu_{25}Fe_{12.5}$, (b) i-$Al_{68}Pd_{23}Mn_9$ and (c) i-$Al_{70.5}Pd_{21}Re_{8.5}$, calculated using the Kramers-Kronig analysis of the loss functions.

7 eV appears clearly even when the shoulder at 23–24 eV is invisible, suggesting it does not come from contamination but is intrinsic to the material.

It is interesting to evaluate the dielectric constants, since the different contributions to it (intra/interband transitions) are additive and can be more conveniently discussed. In Figure 2 we show the real and imaginary parts of the dielectric functions evaluated using the Kramer-Kronig transformation as described in Section 2. We observe an essentially metallic like behaviour, with $\mathrm{Im}(\varepsilon(E))$ decreasing and $\mathrm{Re}(\varepsilon(E))$ increasing and changing sign at the large peak position. Superimposed is a structure around 7 eV related to the bump seen in the spectra, which presumably corresponds to interband transitions. The sharp dip seen in $\mathrm{Im}(\varepsilon(E))$ for i-AlPdRe around 3 eV should be considered with caution, since it depends significantly on the low energy extrapolation of the loss spectrum.

4 Discussion

4.1 Plasmons in icosahedral quasicrystals

As indicated above, the curves shown in Figure 2 may naturally be interpreted in a simple manner. They correspond to a typical metallic behaviour ($\mathrm{Re}(\varepsilon(E))$ and $\mathrm{Im}(\varepsilon(E))$ monotonously increasing (respectively decreasing) when the energy is increased) on which a contribution coming from interband transitions is superimposed. The main peak observed in the loss spectra corresponds to the excitation of a volume plasmon, occurring as expected near the frequency where $\mathrm{Re}(\varepsilon(E)) \sim 0$ and $\mathrm{Im}(\varepsilon(E))$ is small. These behaviours are very similar to the ones obtained in i-Al-Cu-Ru by Terauchi *et al.* [8] as well as on decagonal phases [9]. We can compare our data on i-Al-Pd-Mn with those of Zurkirch *et al.* who measured reflection EELS spectra on i-Al-Pd-Mn surfaces [7]. Their spectra are similar to ours but in their case the main loss peak is situated around 19 eV, instead of 16.8 eV in our case. In other measurements performed in similar conditions (reflection EELS measurements on UHV prepared single grain i-Al-Pd-Mn surfaces), results identical to ours were obtained [18], so the cause of the discrepancy in the loss energies is not clear. In [7] the contributions from the interband transitions to the dielectric constants are also much more pronounced, especially the initial rise of $\mathrm{Im}(\varepsilon)$ above 1 eV. These features strongly depend on the substraction of the zero loss peak from the loss spectrum and on the extrapolations performed at low energy. In our case, we could not identify three distinct low energy structures in i-Al-Pd-Mn.

The values observed for the plasmon energies (position of the loss function maximum) are in the range expected for these alloys, treating the valence electrons as free electrons. Only counting the "*sp*" electrons of the elements the free electron formula gives $\hbar\omega_\mathrm{p} \sim 14.5$ eV. The difference with the actual value may be ascribed to the effect of the other electrons: contribution of the "*d*" electrons of the transition elements and polarization effects of the core electrons. It is indeed well-known that the position of a free electron plasmon can be significantly shifted by the presence of a nearby interband transition.

In [7] a different interpretation of the spectrum of i-Al-Pd-Mn was given. It was argued that the main loss observed there at 19 eV is related to an interband transition involving the Pd "*d*" states, and not to a "quasi free electron plasmon", as opposed to the case of the Al_3Pd alloy to which the quasicrystal was compared. Before

discussing in more details the interpretations of the spectra, we first recall a general point for clarity.

An *intense* loss peak as the ones we observe in the alloys corresponds to a high value of $\mathrm{Im}(-1/\varepsilon(E))$, so to low values of $\mathrm{Re}(\varepsilon(E))$ and $\mathrm{Im}(\varepsilon(E))$, which is precisely the conditions for the existence of a free plasma oscillation. The oscillation may mainly involve free electrons in a metal or "bound" electrons (plasmons so called "associated" to interband transitions). A semiconductor (like pure silicon) may have a well defined free electron like plasmon involving its valence electrons as long as their density is sufficient for the relation $h\omega_\mathrm{p} \gg E_\mathrm{gap}$ to hold [11]. Thus the very low DC electrical conductivity and density of states at the Fermi energy of the stable icosahedral quasicrystals by no means imply that no free electron like plasmon excitation can exist. While the DC conductivity is related to the zero frequency dielectric constant, plasmon oscillations are due to the behaviour of $\varepsilon(E)$ at rather high energies (typically 15 eV) related to the high electron density of the alloys. Thus no marked difference between simple crystalline alloys and decagonal and icosahedral quasicrystals can *a priori* be expected on these grounds.

Coming back to the case of i-Al-Pd-Mn and AlPd alloys, Zurkirch *et al.* relate the main loss peak at 19 eV C and C' (Fig. 2 of [7]) to the interband transitions c and c' seen in $\mathrm{Im}(\varepsilon(E))$. In our case, considering sum rules, it does not seem plausible to assign the main loss peak only to one of the structures seen at low energy in $\mathrm{Im}(\varepsilon)$. Sum rules state that the integrals $I_1 = f\,\mathrm{Im}(\varepsilon(E))E\ \mathrm{d}E$ and $I_2 = f\,\mathrm{Im}(-1/\varepsilon(E))E\ \mathrm{d}E$ evaluated on the whole energy range are equal and proportional to the total number of electrons participating in the spectra. We can evaluate the contribution of the bump seen in the $\mathrm{Im}(\varepsilon(E))$ spectrum of i-Al-Pd-Mn between 5 eV and 15 eV. The value cannot be computed precisely since it depends on the low energy extrapolations performed on the experimental loss spectrum, but it is found to be smaller than 100 eV^2. When calculating the contribution of the main loss peak (between 10 eV and 25 eV) to I_2 one gets a value of 300 eV^2. Although one should be cautious when using sum rules in limited energy ranges, this difference in magnitude is significant, and it is quite improbable that only (a part of) the bump seen in $\mathrm{Im}(\varepsilon(E))$ at low energy gives rise to the main loss peak. We rather suggest that the metallic like background of $\mathrm{Im}(\varepsilon(E))$ mainly contributes to it. Applying the sum rules to the entire experimental energy range (0–38 eV) gives $I_1 \approx I_2 \approx 450$ eV^2. These facts are consistent with a "s–p electron" plasmon interpretation of the EELS curves of i-Al-Pd-Mn. The same discussion also applies to the other alloys, which spectra are very similar, irrespective of the nature of the transition metals present.

We may also apply the same comments to the case of Al_3Pd (Fig. 3 of [7]) with the difference that the energies of the interband transitions are higher and closer to the "free electron like" plasmon, causing its asymetry. Note that in that case, the peak B cannot correspond to a surface plasmon (as suggested by the comparison with pure Al), since if this was true it should not appear in $\mathrm{Im}(\varepsilon(E))$ (no peak b).

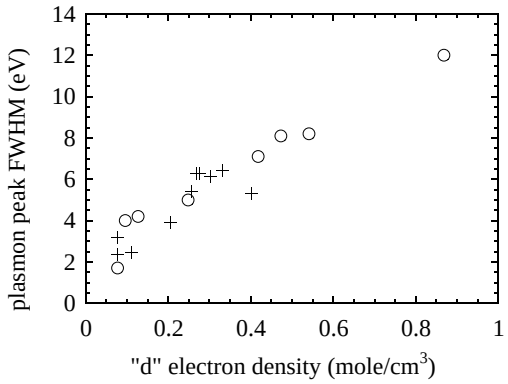

Fig. 3. Plasmon peak width at half maximum of: i) crystalline binary Al-Transition Metal alloys, from [4,19], (o); ii) icosahedral and decagonal quasicrystals from this paper and [3–5,8,9] (+). Data are plotted as a function of the "*d*" electron density. In order of increasing "*d*" electron density: orth.Al_6Mn, TiAl, V_5Al_8, Co_2Al_5, Ni_2Al_3, CoAl, NiAl, Ni_3Al (o); i-Al_6Mn, i-$Al_{74}Mn_{20}Si_6$, i-$Al_{75}Cu_{15}V_{10}$, d-$Al_{70}Co_{15}Ni_{15}$, d-$Al_{70}Ni_{20}Rh_{10}$, i-$Al_{70.5}Pd_{21}Re_{8.5}$, i-$Al_{68}Pd_{23}Mn_9$, i-$Al_{65}Cu_{20}Ru_{15}$, i-$Al_{62.5}Cu_{25}Fe_{12.5}$ (+).

4.2 Plasmon width

The full width at half maximum (FWHM) $\delta E_{1/2}$ of the plasmon peaks we observe is quite large (see Tab. 1). It is much higher than what is observed for simple metals (aluminum, alcalines) for which one typically has $\delta E_{1/2} <$ 1 eV, and is also higher than for semiconductors (Si,...) where $\delta E_{1/2} \sim 4$ eV. It is well-known that the main contribution to plasmon broadening at low wave vector is its decay into interband transitions. Broad interband transitions situated in the vicinity of the plasmon energy result in a strong damping of it. This situation is expected with aluminum-transition metals alloys due to the interband transitions involving the "*d*" electrons. It was shown in binary alloys [19] that the plasmon width $\delta E_{1/2}$ increases with the concentration of the transition metals. In the case of Al-Co, Al-Ni and Al-Cu alloys containing from 60% to 70% of aluminum, plasmon width ranging from 4 eV to 6 eV were observed. In Figure 3 we plot the plasmon FWHM of crystalline binary alloys, together with those of icosahedral and decagonal quasicrystals, as a function of the density of "*d*" electrons n_d. For i-Al-Pd-Re, the "*f*" electrons of the Re atoms were neglected, their binding energy being much higher than the plasmon energy. The plasmon width is seen to correlate remarkably and increases linearly with n_d. A similar trend was already noted for i-Al-Cu-Ru and decagonal quasicrystals [9]. In a phenomenological description, $\delta E_{1/2}$ is proportional to $\mathrm{Im}(\varepsilon(E_\mathrm{p}))$. Supposing that the "*d*" electron interband transitions give contributions to $\mathrm{Im}(\varepsilon(E_\mathrm{p}))$ that depend mainly on their intensities, and not much on their energy position, then the observed linear increase of $\delta E_{1/2}$ with n_d is expected. The scattering of the points may be attributed to the different conditions in which the FWHM values where extracted from the experimental data, as well as to deviations from that simple hypothesis. But the observation of the correlation gives a good indication

that the main loss peak in quasicrystals is a $s-p$ plasmon damped *via* the excitation of the "*d*" electrons of the transition metals.

5 Conclusion

We have studied the electron energy loss spectra of icosahedral quasicrystals in the 0–40 eV range. These are dominated by a plasmon loss, which energy and line shape do not depend much on the alloy studied. The data are consistent with a "$s-p$ electron plasmon", its broadening being due to interband transitions involving the "*d*" electrons of the transition elements. It increases with their density, and is of the same order as in other non quasicrystalline Al-transition metal systems. No strong feature related to the quasicrystalline order thus appears. The determination of the loss function of the quasicrystals down to a few eV should be helpful to improve the numerical treatment of the optical data of these alloys.

We are very grateful to M. de Boissieu for providing the i-AlPdMn sample, and to A. Filhol and T. Stöckli for providing us with the "ABFfit" and Kramers-Krönig softwares respectively.

References

1. C. Berger, in *Lectures on quasicrystals*, edited by F. Hippert, D. Gratias (Les Éditions de Physique, Les Ulis, 1994); S. Roche, G. Trambly de Laissardière, D. Mayou, J. Math. Phys. **38**, 1794 (1997).
2. D.N. Basov *et al.*, in *Proceedings of the 5th International Conference on Quasicrystals, Avignon, 1995*, edited by R. Mosseri, C. Janot (World Scientific, Singapore, 1995), p. 564; and the references therein.
3. C.H. Chen, D.C. Joy, H.S. Chen, J.J. Hauser, Phys. Rev. Lett. **57**, 743 (1986).
4. J.L. Verger-Gaugry, P. Guyot, J. Phys. Colloq. France **47**, C3-477 (1986); J.L. Verger-Gaugry, P. Guyot, M. Audier, Phys. Lett. A **117**, 307 (1986).
5. L.E. Levine, P.C. Gibbons, K.F. Kelton, Phys. Rev. B **40**, 9338 (1989).
6. M. Zurkirch, A. Atrei, M. Hochstrasser, M. Erbudak, A.R. Kortan, J. Electron Spectrosc. Relat. Phenom. **77**, 233 (1996); M. Zurkirch, M. De Crescenzi, M. Erbudak, M. Hochstrasser, Phys. Rev. B **55**, 8808 (1997).
7. M. Zurkirch, M. De Crescenzi, M. Erbudak, A.R. Kortan, Phys. Rev. B **56**, 10651 (1997).
8. M. Terauchi, M. Tanaka, A.P. Tsai, A. Inoue, T. Masumoto, Phil. Mag. Lett. **74**, 107 (1996).
9. M. Terauchi, H. Ueda, M. Tanaka, A. Tsai, A. Inoue, T. Masumoto, Phil. Mag. Lett. **77**, 351 (1998); M. Terauchi, H. Ueda, M. Tanaka, A. Tsai, A. Inoue, T. Masumoto, Phil. Mag. Lett. **77**, 1625 (1998).
10. T. Klein, C. Berger, D. Mayou, F. Cyrot-Lackmann, Phys. Rev. Lett. **66**, 2907 (1991); C. Gignoux, C. Berger, G. Fourcaudot, J.C. Grieco, H. Rakoto, Europhys. Lett. **39**, 171 (1997).
11. H.Rather, *Excitation of plasmons and interband transitions by electrons* (Springer-Verlag, Berlin, 1980).
12. R.F.Egerton, *Electron Energy Loss Spectroscopy in the electron microscope* (Plenum Press, New-York, 1986).
13. A. Antoniadis, J. Berruyer, A. Filhol, *Affinement de spectres par une méthode du maximum de vraisemblance*, Rapport de contrat ILL/ SAD-AF-CT 85-229 et ILL/ SAD-AF 24, 1988.
14. T. Stöckli, *Étude des propriétés électroniques de particules d'aluminium et de nanotubes de carbone par EELS*, Mémoire de thèse, École Polytechnique de Lausanne, 1995.
15. U. Bangert, A.J. Harvey, R. Keyse, Ultramicroscopy **68**, 173 (1997).
16. P.M. Ajayan, S. Iijima, T. Ichihashi, Phys. Rev. B **47**, 6859 (1993).
17. R.W. Ditchfield, Solid State Commun. **19**, 443 (1976).
18. F. Schmittusen, J. Chevrier (private communication).
19. O. Klemperer, J.P.G. Shepherd, Brit. J. Appl. Phys. **14**, 89 (1963); E.A. Bakulin, M.M. Bredov, V.A. Vasil'ev, Sov. Phys.-Solid State **13**, 2536 (1972).